Acid-triggered radical polymerization of vinyl monomers

Check for updates

Maria-Nefeli Antonopoulou [1], Glen R. Jones [1], Asja A. Kroeger [2,3], Zhipeng Pei [2], Michelle L. Coote [2] ✉, Nghia P. Truong [1,4] ✉ & Athina Anastasaki [1] ✉

Reversible addition–fragmentation chain-transfer (RAFT) polymerization is one of the most versatile and robust controlled radical polymerization methods owing to its broad material scope and high tolerance to various functionalities and impurities. However, to operate RAFT polymerization, a constant supply of radicals is required, typically via exogenous thermal radical initiators that are not only challenging to transport and store, but also primarily responsible for termination and end-group heterogeneity. Here we present an acid-triggered RAFT polymerization that operates in the dark and without any conventional radical initiator. Abundant acids (for example, sulfuric acid) are shown to have a dual role initiating and accelerating the polymerization. The polymers prepared have low dispersity and high end-group fidelity. The method is compatible with a wide range of vinyl monomers and solvents, and can be applied to the synthesis of well-controlled high molecular weight block copolymers, as well as to free radical polymerization.

Reversible-deactivation radical polymerization methodologies, such as atom transfer radical polymerization (ATRP)[1–3], nitroxide-mediated polymerization[4] and reversible addition–fragmentation chain-transfer (RAFT) polymerization[5,6], enable the synthesis of tailor-made polymers with controlled molecular weight, dispersity and architecture[7–10]. Among them, RAFT is one of the most versatile owing to its ability to polymerize an extensive range of monomer classes, and as such it has been largely adopted to generate a wide variety of materials[6]. The attractiveness of RAFT lies in its mechanism, which can be thought of as a free radical polymerization (FRP) in the presence of a reversible chain-transfer agent (CTA). Through a degenerative chain-transfer mechanism the propagating species equilibrate with dormant species via a thiocarbonylthio compound, also referred to as a RAFT agent[11]. It is noted that propagating radicals are terminated during RAFT polymerization and the degenerative chain-transfer process does not create new radicals. As such, an external radical source is typically required to initiate the polymerization and also ensure a sufficient supply of radicals to achieve high conversions and polymerization rates[12,13].

However, the necessity to use exogenous thermal radical initiators poses certain restrictions. First, the extent of termination in a RAFT polymerization is directly proportional to the amount of radical initiator employed[12]. Unlike ATRP and nitroxide-mediated polymerization that operate through a reversible termination mechanism[4,14], the RAFT process does not prevent the formation of dead chains[15,16]. As a result, the use of radical initiators leads to end-group heterogeneity (for example, initiator-derived chains and RAFT-derived chains) and terminated chains. Such termination is further exemplified in the synthesis of block copolymers as a new aliquot of radical initiator is introduced together with the next monomer addition, thus leading to the gradual accumulation of terminated chains and resulting in higher dispersities and impure block copolymers[17]. Another consideration of commonly employed thermal radical initiators, such as peroxides and azo-compounds, is that they are highly explosive chemicals and as such quite challenging to not only transport but also to store[18–21]. In fact, this is an issue not only for RAFT polymerization but also for FRP, one of the most common polymerization methodologies in industry. Therefore, eliminating the use of

[1]Laboratory of Polymeric Materials, Department of Materials, ETH Zürich, Zürich, Switzerland. [2]Institute for Nanoscale Science and Technology, College of Science and Engineering, Flinders University, Bedford Park, South Australia, Australia. [3]Research School of Chemistry, Australian National University, Canberra, Australian Capital Territory, Australia. [4]Monash Institute of Pharmaceutical Sciences, Monash University, Parkville, Victoria, Australia. ✉e-mail: michelle.coote@flinders.edu.au; nghia.truong@monash.edu; athina.anastasaki@mat.ethz.ch
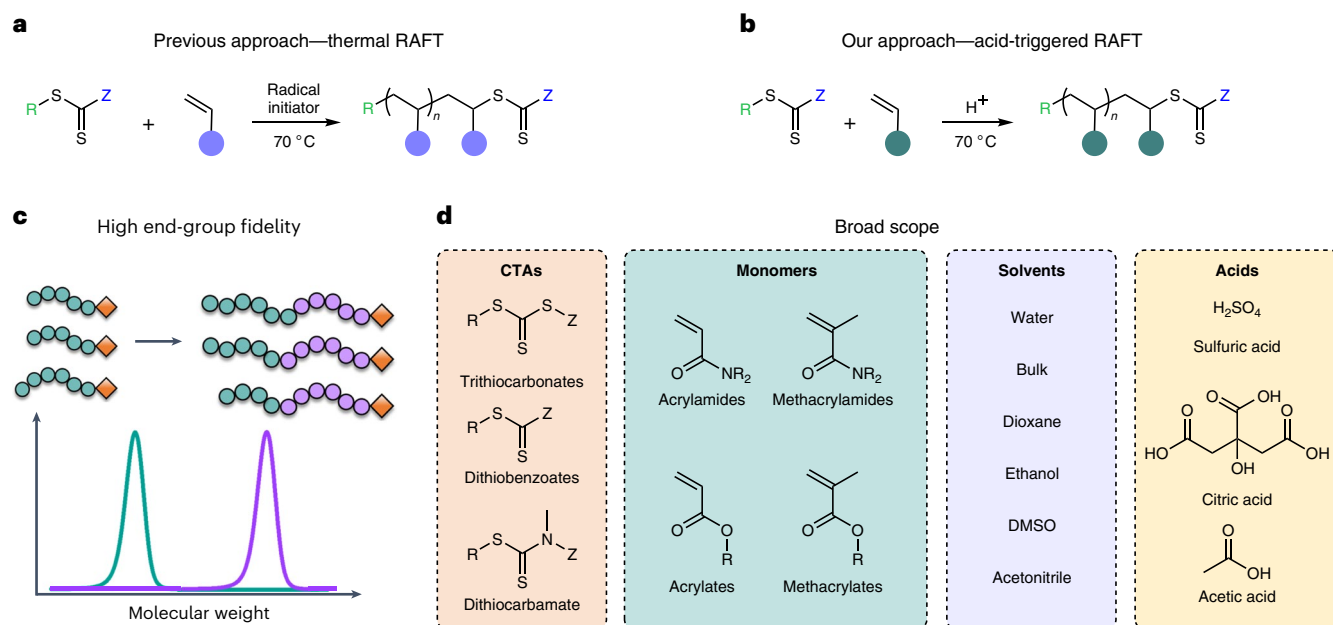
Fig. 1 | Acid-triggered RAFT polymerization with a broad scope and high end-group fidelity. a,b, Conventional thermal RAFT polymerization[12] (**a**) and acid-triggered RAFT polymerization (**b**). **c,d**, High end-group fidelity furnished by acid-triggered RAFT polymerization exemplified by chain extensions (**c**), and the broad scope of the technique including a wide range of CTAs, monomers, solvents and acids (**d**).

thermal radical initiators would be highly beneficial to not only enhance the quality of the synthesized polymers but also to overcome transportation and storage issues. Some of the limitations of conventional thermal RAFT polymerization have been alleviated with the emergence of photo-mediated polymerization processes such as photoinduced electron/energy transfer RAFT[22,23] or photo-iniferter polymerizations[23–26]. In addition, Matyjaszewski and coworkers have explored the possibility of using ATRP copper complexes to activate RAFT agents[27–30]. Yet, conventional thermal RAFT remains a very attractive polymerization methodology primarily due to its simple setup, compatibility with a wider monomer scope, the potential to synthesize well-defined block copolymers and the relative ease of scale-up[13,31–33].

In this Article, we report an acid-triggered RAFT polymerization methodology that does not require light or thermal radical initiators. In the presence of low concentrations of highly abundant strong (for example, sulfuric) or weak (for example, citric) acids, a wide range of monomer classes (for example, (meth)acrylates and (meth)acrylamides) can be polymerized in a controlled fashion in both aqueous and organic media yielding well-defined polymers with narrow molar mass distributions and high end-group fidelity (Fig. 1). The dual role of the acid to not only initiate the polymerization but also to accelerate the reaction rate allows for the synthesis of high molecular weight homo and block copolymers with reduced termination. In addition, our approach is compatible with conventional radical polymerization, omitting the need to use highly explosive thermal initiators and rendering the methodology more widely applicable.

Results and discussion
Acid-triggered RAFT polymerization
The acid-triggered polymerization of vinyl monomers was fortuitously discovered during the thermal RAFT polymerization of dimethyl acrylamide (DMA). The model reaction was composed of 2-(((butylsulfanyl) carbothioyl)sulfanyl)propanoic acid (PABTC, CTA 1, 1 equiv.) as the RAFT agent, DMA as the monomer (500 equiv. with respect to the CTA), water as the reaction medium and sulfuric acid as a highly abundant acid (10 equiv.) (Fig. 2a). The pH of the solution was measured at 1.7. In the absence of any conventional radical initiator and upon deoxygenation,

the solution was heated at 70 °C and the reaction was allowed to commence. [1]H nuclear magnetic resonance (NMR) spectroscopy confirmed 90% monomer conversion in 10 h while size exclusion chromatography (SEC) revealed a symmetric molar mass distribution with $Đ = 1.13$ (Supplementary Fig. 1). As a control experiment, we attempted to polymerize DMA without acid but no conversion was detected by ^{1}H NMR, even after 3 days. These results suggest that neither the RAFT agent nor the monomer (for example, through autoinitiation) alone can be responsible for the initiation of the polymerization in the presence of acid. It is important to note that this acid-triggered polymerization operates in the absence of a conventional initiating system (for example, thermal initiation, photoinitiation, redox initiation and ionizing radiation).

To gain a deeper insight into this highly unusual reaction, we undertook a series of kinetic studies at various pH values monitored in situ by ^{1}H NMR spectroscopy at 70 °C (Fig. 2b). In comparison with conventional batch sampling methods, this approach is uniquely suited to study fast reaction kinetics as it ensures sufficient time points throughout the polymerization, and permits accurate measurements to be taken without disturbing the reaction through continuous and potentially deleterious sampling[34]. At pH 6.5, the pH of the monomer and CTA aqueous solution (that is, no acid was added), no monomer conversion was detected, in line with the batch experiment, as shown in Fig. 2b, Supplementary Fig. 2 and Supplementary Table 1. When 0.1 equiv. with respect to the CTA was added (pH 5.2), the reaction was successfully triggered and a controlled polymerization took place producing a well-defined poly(dimethylacrylamide) (PDMA) ($Đ = 1.12$) with just 20 ppm of sulfuric acid. The possibility to conduct a RAFT polymerization at such low concentrations of a highly abundant acid further highlights the simplicity of our methodology. Upon gradually increasing the amount of acid to 0.15 equiv. (pH 4.7) and 0.65 equiv. (pH 3.0), faster polymerization rates were monitored without compromising the control over the polymerization (Fig. 2c and Supplementary Table 1). However, at higher acid concentrations (pH 1.7, 10 equiv.), no further increase in the reaction rate was observed. Overall, these kinetic experiments suggest that the rate of radical formation correlates with the amount of the acid added until a threshold is reached, after which no appreciable change in the polymerization rate is recorded.
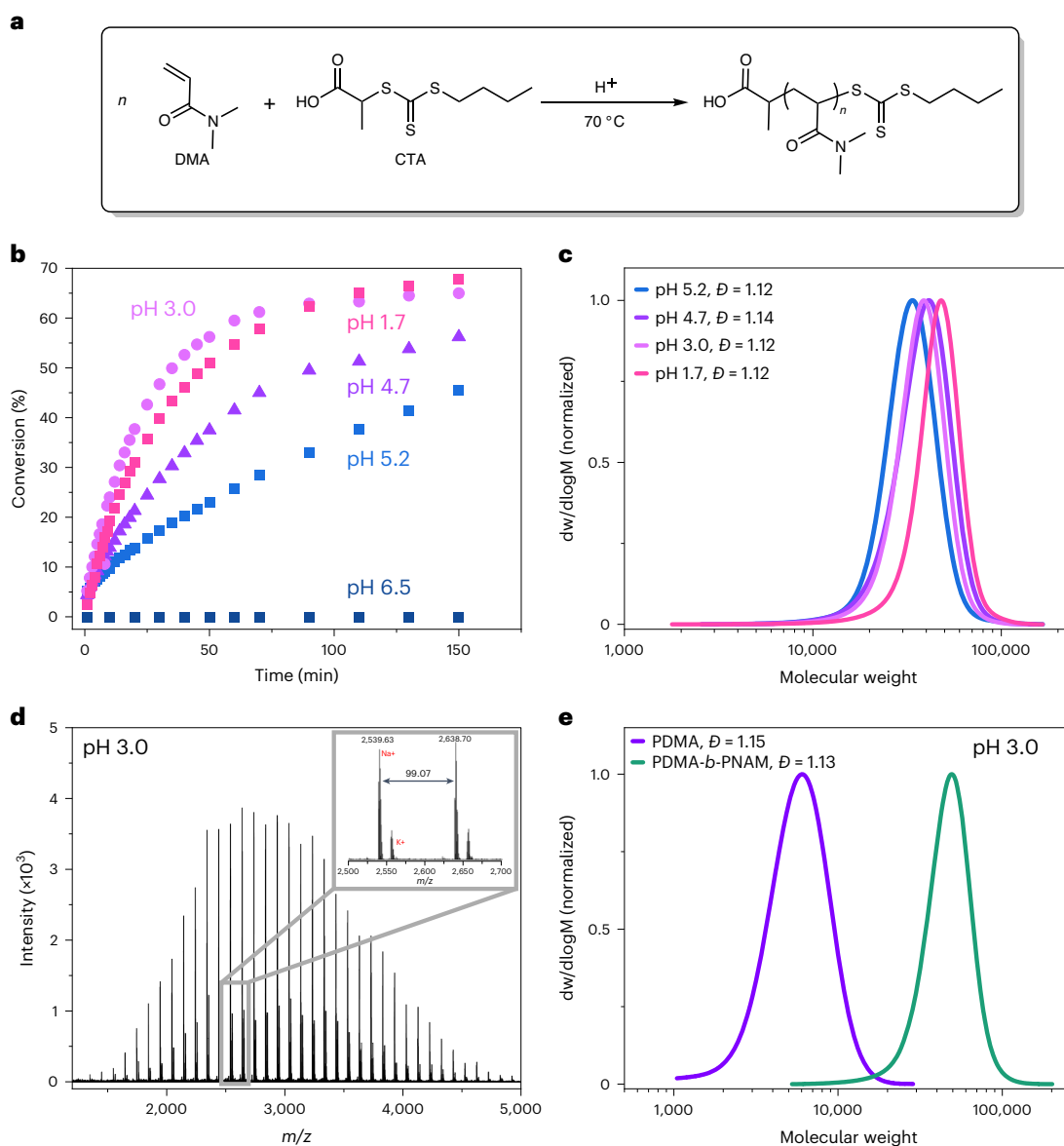
Fig. 2 | An overview of acid-triggered RAFT polymerization of DMA. a, Scheme showing acid-triggered RAFT polymerization of DMA. **b**, Kinetic profiles of PDMA in water in 20/80 v/v at different pHs, with different acid ratios with respect to the CTA; pH 6.5, 0 equiv., pH 5.2, 0.1 equiv., pH 4.7, 0.15 equiv., pH 3.0, 0.65 equiv., pH 1.7, 10 equiv. **c**, SEC trace representing the molar mass distributions at the end of the polymerizations shown in **b**. **d**, MALDI-ToF MS illustrating the results for a PDMA homopolymer capped with the CTA ($C_3H_5O_2S_3$ (($CH_2CHCON(CH_3)_2)_{23}$) ($C_3H_5O_2$), **e**, Chain extension of PDMA homopolymer with NAM via acid addition.

Considering that sulfuric acid is a strong acid, we also examined the possibility of CTA degradation during the polymerization. A lower molecular weight PDMA was synthesized at pH 3 ($M_n = 3,000$, $Đ = 1.12$) and subsequently analysed by matrix-assisted laser desorption ionization time-of-flight mass spectrometry (MALDI-ToF MS). Pleasingly, a single polymeric species was observed (Na$^+$ and K$^+$ adduct) corresponding to the expected PDMA functionalized with CTA at both chain ends while no sign of CTA degradation was detected (Fig. 2d). In addition, when PDMA was chain-extended with *N*-acryloylmorpholine (NAM), the molar mass distribution clearly shifted to higher molecular weights yielding a well-defined PDMA-*b*-(poly(*N*-acryloylmorpholine)) (PNAM) diblock copolymer ($Đ = 1.13$; Fig. 2e and Supplementary Table 2). Taken altogether, these results suggest that acid-triggered RAFT polymerization leads to polymers with very high end-group fidelity due to side reactions and termination events being substantially suppressed.

Intrigued by this high end-group fidelity, we were interested in comparing our acid-triggered RAFT polymerization with conventional thermal RAFT polymerization. To exaggerate any potential differences between the two systems we targeted the synthesis of a relatively high molecular weight homopolymer (degree of polymerization (DP) 1,000). Optimized thermal RAFT was conducted at 70 °C in the presence of 0.03 equiv. of 2,2′-azobis(2-(2-imidazolin-2-yl)propane) dihydrochloride (VA-044) as the radical initiator, resulting in PDMA with $Đ = 1.45$ (Supplementary Fig. 3 and Supplementary Table 3). It is noted that 0.03 equiv. was the minimum amount of VA-044 required to reach relatively high monomer conversion (79%). Instead, when our acid-triggered RAFT polymerization approach was employed (10 equiv. of sulfuric acid, pH 2), narrower molar mass distributions ($Đ = 1.13$) were obtained at comparable monomer conversions (87%), highlighting the superiority of our approach over traditional thermal RAFT polymerization. To probe the potential of this technique in maintaining high end-group fidelity in block copolymer synthesis, we subsequently targeted the one-pot synthesis of high molecular weight triblock copolymers with each block set at DP 200 (Fig. 3a). It is noted that the synthesis of such
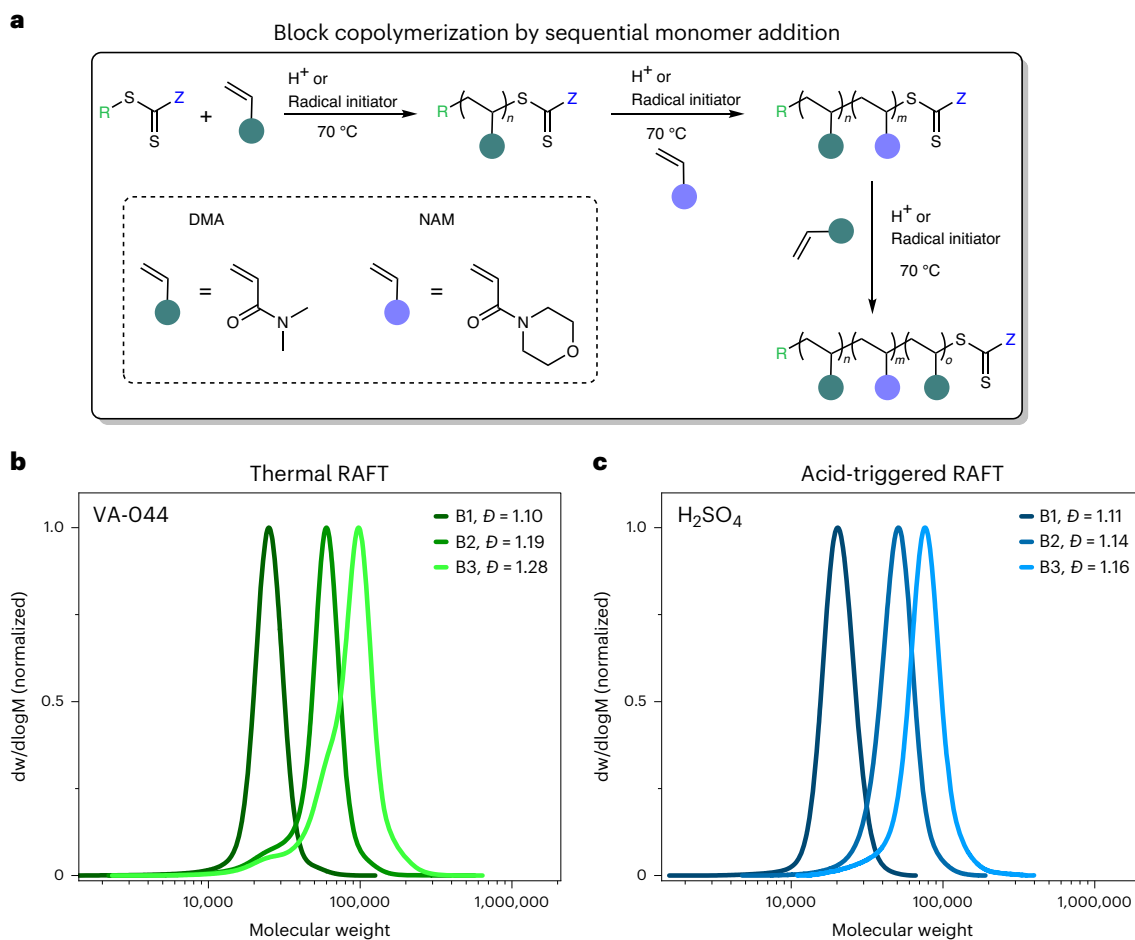
Fig. 3 | Synthesis of triblock copolymers via conventional and acid-triggered RAFT polymerization. a, One-pot triblock copolymer synthesis through iterative monomer addition with either VA-044 or sulfuric acid. **b,c**, SEC traces representing triblock copolymers of acrylamides initiated by VA-044 (**b**) and sulfuric acid (**c**). dw/dlogM is the normalized distribution of slice molecular weights.

high molecular weight block copolymers is rarely attempted by RAFT polymerization in the literature owing to the large extent of termination that gradually accumulates in the system[35]. Indeed, optimized thermal RAFT polymerization resulted in a triblock copolymer with a final $Đ$ of 1.28 in which obvious low molecular weight tailing could be observed by SEC as the main polymer distribution shifted to higher molecular weights (Fig. 3b and Supplementary Table 4). In contrast, when acid-triggered RAFT polymerization was employed, the final $Đ$ of the triblock was maintained at 1.16 with substantially less tailing observed (Fig. 3c and Supplementary Table 5). The differences in end-group fidelity between the two methods indicate that the acid may potentially possess a dual role and is not only responsible for the generation of radicals.

Mechanism and application to FRP

To get a clearer picture of the mechanism, we conducted a number of experiments in the absence of a RAFT agent, a process analogous to conventional FRP but without an initiator. Upon deoxygenating an aqueous mixture of DMA at 70 °C, no monomer conversion was detected by ^{1}H NMR (Fig. 4b, pH 6.6, Supplementary Table 6) even after 72 h, suggesting that no autopolymerization occurs in the absence of acid. However, the presence of just 32 ppm of sulfuric acid (pH 5.5, no CTA and initiator added; Fig. 4a and Supplementary Table 6) led to a rapid FRP yielding PDMA with $M_n = 800,000$ exhibiting a broad, yet relatively symmetrical, molar mass distribution ($Đ = 2.0$; Fig. 4c). In line with the acid-triggered RAFT polymerizations, addition of further acid led to a gradual acceleration of the reaction rate until a threshold was

reached around pH 4.5, as seen in Fig. 4b. Increasing the acid content further (pH ≤4.5), did not result in faster polymerization rates. It is noted that comparable molecular weights and dispersities were reproducibly observed regardless of the amount of acid employed. Interestingly, when the identical experiments were conducted in the presence of a free radical initiator (no acid added), substantially lower molecular weights ($M_n = 200,000$) and broader molar mass distributions ($Đ > 4$) were obtained, as seen in Supplementary Fig. 4 and Supplementary Table 7. The higher molecular weights and lower dispersities obtained by acid-triggered FRP are attributed to less primary termination (that is, growing macroradicals terminated by azo-initiator-derived radicals)[36]. We also conducted a range of acid-triggered FRPs at various temperatures and calculated the activation energy, which was found to be 39.1 kJ mol^{-1} (Supplementary Fig. 5 and Supplementary Table 8).

Collectively, these findings demonstrate that highly abundant acids can trigger an efficient radical polymerization that not only occurs in the absence of explosive chemicals but also improves the quality of the synthesized polymers by suppressing termination. The obtained data also exclude the possibility of any potential interactions of the acid with the RAFT agent and point towards an acid-triggered autoinitiation mechanism[37] that involves direct interactions of the monomer with the acid. Considering that no autopolymerization was observed for DMA at 70 °C in the absence of acid, conventional autopolymerization can be precluded. The polymerization is almost certainly radical in nature as cationic pathways can be excluded since water was used as the reaction medium[38]. Acrylic monomers are known

a

b

c

d

e
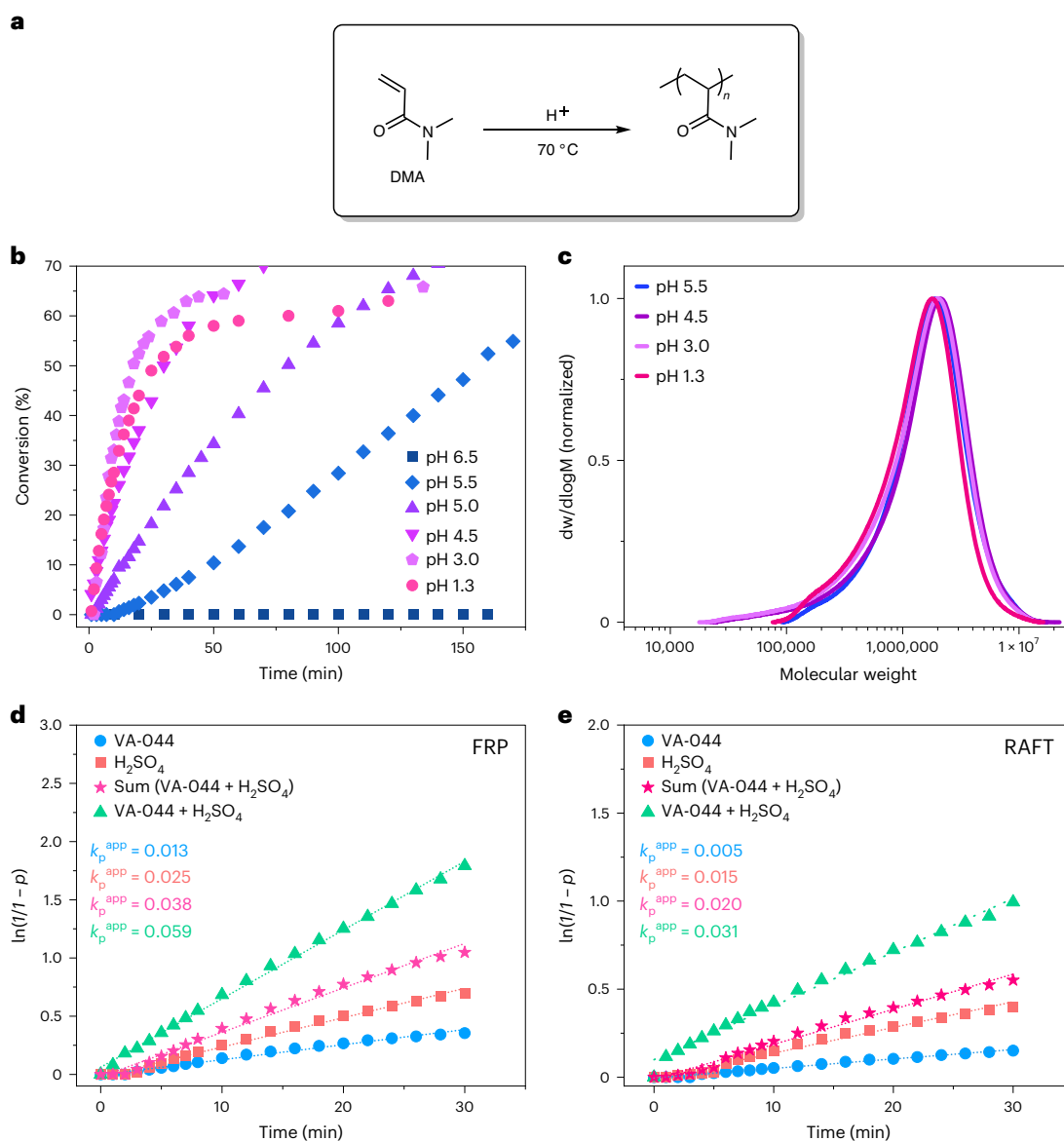
Fig. 4 | Acid-triggered FRP and the rate-enhancing effect of acid. a, FRP of DMA in water initiated by acid. **b,** Kinetic profiles of acid-triggered FRPs with varying pH. **c,** SEC traces representing the molar mass distributions at the end of the polymerizations. **d,** Pseudo-first order kinetic plots of aqueous FRPs of DMA demonstrating the rate-enhancing effect of acid. **e,** Pseudo-first order kinetic plots of aqueous RAFT polymerizations of DMA demonstrating the rate-enhancing effect of acid. 'p' denotes conversion.

to undergo autoinitiation at high temperatures (>200 °C) via a Flory-type autoinitiation mechanism, whereby two monomers react via an open-shell singlet pathway to form diradical species (Fig. 5a)[37,39–41]. However, autoinitiation at lower temperatures has not been reported, and none was observed for DMA at 70 °C in the absence of acid. In addition, the rate of polymerization positively correlates with the amount of acid added to the system and hence the generation of radicals. We thus speculated whether acid might be protonating the monomer and thereby electrostatically catalysing this autoinitiation process. The ability of charged functional groups to stabilize radicals and catalyse radical processes is well known[42–44]. To test this proposal we used density functional theory (DFT) calculations to compare the autoinitiation barriers for DMA in water at 70 °C in the presence and absence of acid. In all cases, autoinitiation was found to proceed through an open-shell singlet transition state, consistent with the Flory mechanism. Various protonation states were considered (Supplementary Fig. 10); all were catalytic, with the most effective, that involving protonation

at nitrogen, leading to an increase in rate of 3.5 orders of magnitude. Based on the computed barrier, the predicted half-life of the catalysed reaction is approximately 82 min, consistent with efficient polymerization at this temperature (Fig. 5b). In line with these calculations, the polymerization of acrylic acid should proceed efficiently in the absence of any externally added acid and without a radical initiator. Indeed, acrylic acid could effectively polymerize at 70 °C yielding 79% monomer conversion while the addition of acid led to a comparable conversion (Supplementary Fig. 6).

Based on theory and experiment, acid thus appears to catalyse autoinitiation of radical polymerization to such an extent that it occurs readily at 70 °C instead of the high temperatures normally required. However, the reaction reaches a threshold at a certain pH value below which no further rate enhancement is observed. As such, the acid may not only be responsible for generating radicals but may potentially play an additional role. This dual role of the acid is further supported by the fact that both RAFT and free radical acid-triggered polymerizations
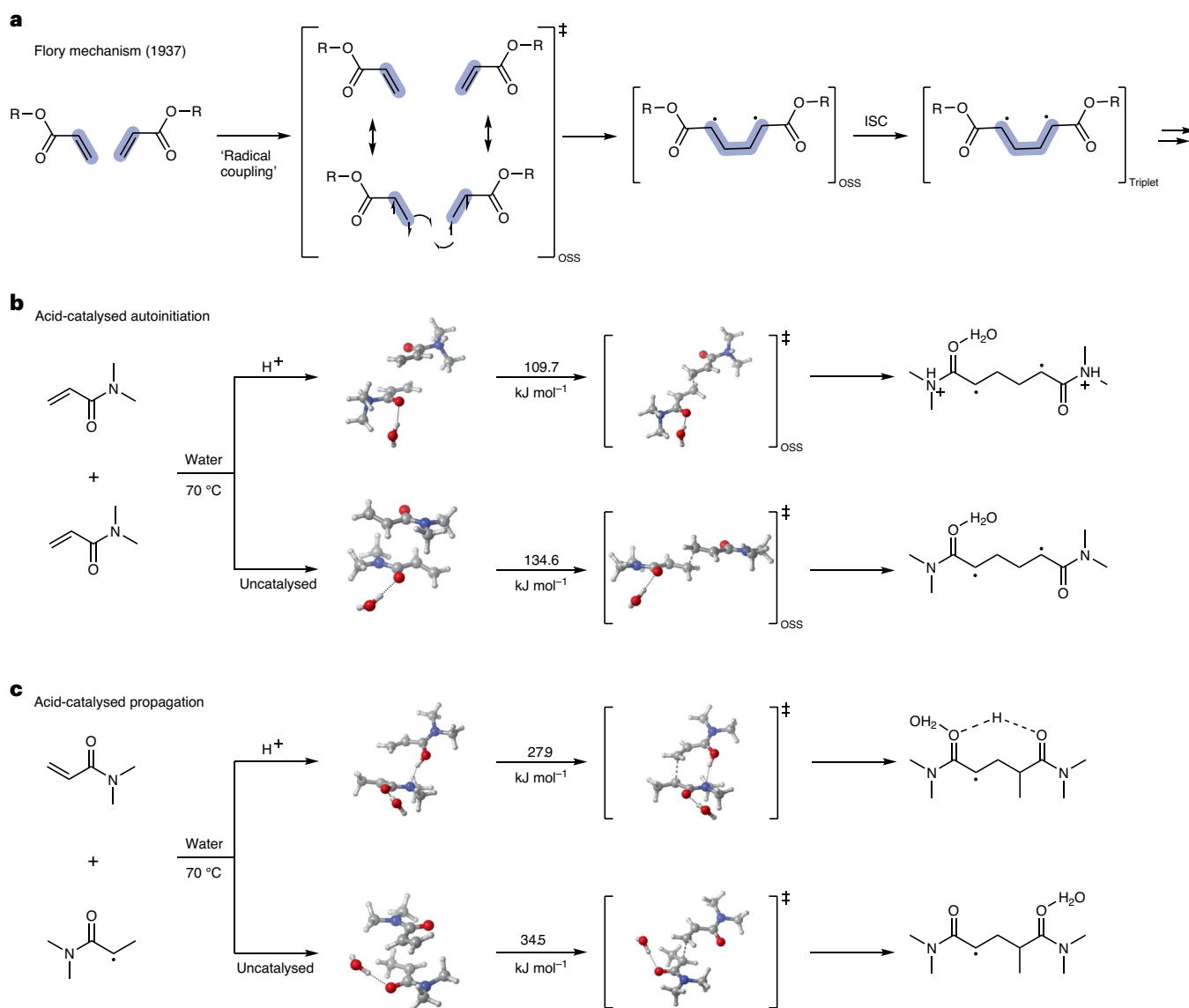
Fig. 5 | Proposed mechanism of catalysis in acid-triggered polymerization. a, Flory mechanism of autoinitiation[37,39–41]. Autoinitiation proceeds through an open-shell singlet (OSS) transition state to afford a diradical intermediate that can undergo intersystem crossing (ISC) to the triplet, which can then undergo polymerization. **b**, Computed Gibbs free energy barriers (70 °C, water) for the rate-determining step in autoinitiation in the presence and absence of acid. Calculations were performed at the wB97X-D/aug-cc-pVTZ//M062X/6-31g(d,p) level of theory using an explicit water molecule combined with the SMD implicit solvent model to model the water environment. Barriers were computed from

the solvated reactant complexes. **c**, Computed Gibbs free energy barriers (70 °C, water) for propagation in the presence and absence of acid. Calculations were performed at the wB97X-D/aug-cc-pVTZ//M062X/6-31g(d,p) level of theory using an explicit water molecule combined with the SMD implicit solvent model to model the water environment. Barriers were computed from the solvated reactant complexes, and for simplicity only a unimeric propagating radical was considered. For additional details including calculations on other protonation states, see Supplementary Figs. 10–14.

exhibit suppressed termination as opposed to traditional approaches in which thermal radical initiators are employed. We propose that the monomer protonation may also lead to an acceleration of the propagation reaction rate, reducing the overall radical concentration required and thus minimizing termination events. A rate acceleration phenomenon has previously been reported in conventional and controlled radical polymerizations with addition of Lewis acids, with DFT calculations indicating an electrostatic origin for the catalytic effect[43,45–49]. Indeed, our DFT calculations indicate that the propagation rate coefficient of DMA at 70 °C in water increases by approximately one order of magnitude upon protonation of the monomer (Fig. 5c).

To further investigate the rate acceleration effect of the acid we conducted additional experiments. First, the FRP of DMA (no acid added) was performed at 70 °C using VA-044 as a thermal radical initiator

(Supplementary Table 9). The recorded apparent rate constant of polymerization (k_p^{app}) was 0.013 min⁻¹. In another reaction, without the addition of a thermal radical initiator, the acid-triggered FRP of DMA gave a k_p^{app} of 0.025 min⁻¹. By then combining the total amount of VA-044 and sulfuric acid previously employed in a single experiment, a k_p^{app} of 0.038 min⁻¹ would be expected assuming that the acid is solely acting as a radical source. Instead, when employing identical concentrations of combined VA-044 and sulfuric acid, a k_p^{app} of 0.059 min⁻¹ was observed, which is appreciably faster than the individual rates combined (Fig. 4d and Supplementary Table 9). This synergistic rate enhancement was also evident at higher VA-044 concentrations, and for acid-triggered RAFT polymerization (Fig. 4e and Supplementary Table 9). A similar rate enhancement was also observed when PEG acrylate was polymerized, thus suggesting that this effect is not limited to acrylamides
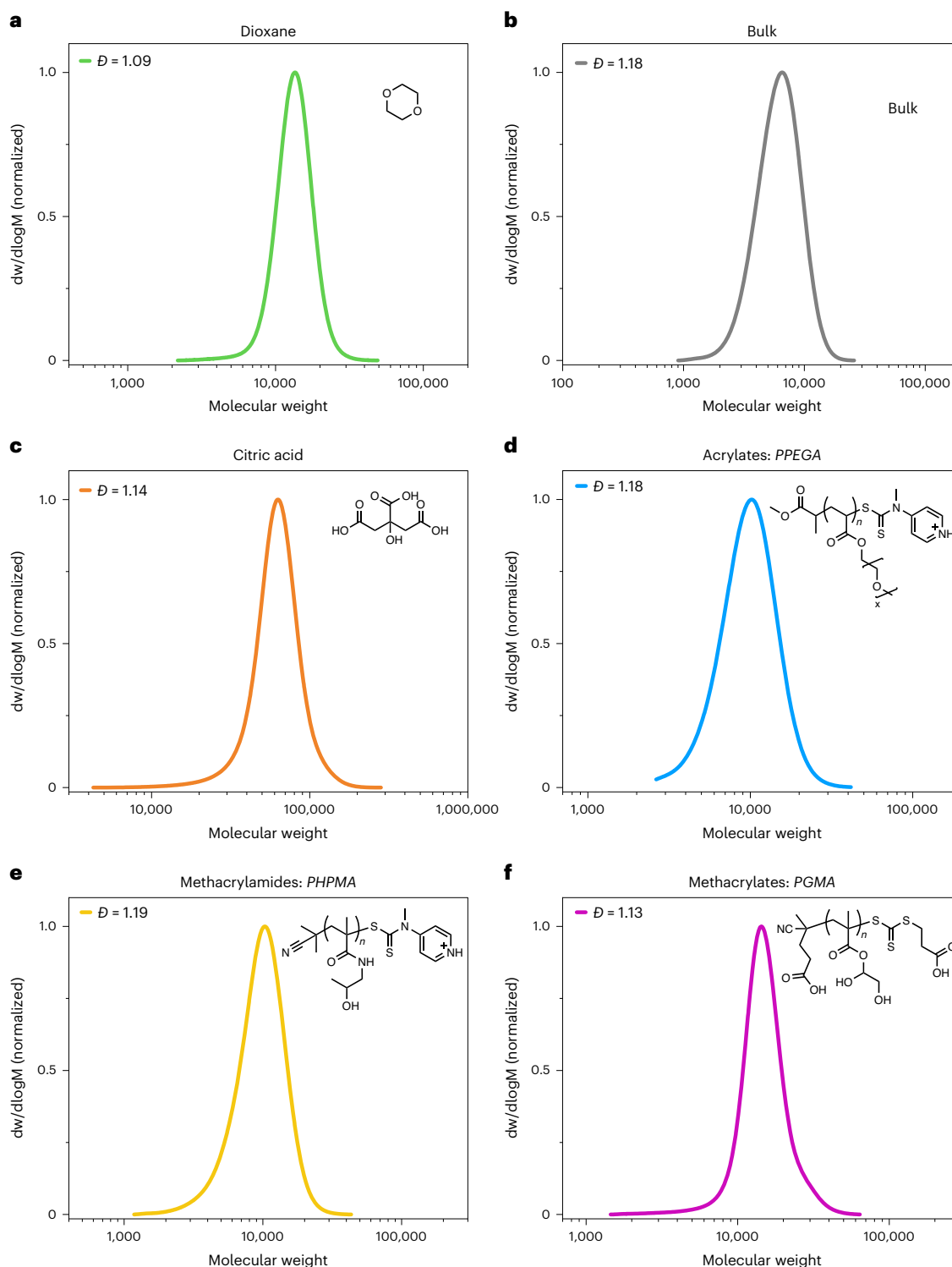
Fig. 6 | Selected SEC spectra demonstrating the scope of acid-triggered RAFT polymerization. a, Polymerization of NAM in dioxane. **b**, Polymerization of NAM under bulk conditions. **c**, Aqueous polymerization of NAM triggered by citric acid. **d**, Aqueous polymerization of PEGA. **e**, Aqueous polymerization of HPMA. **f**, Aqueous polymerization of GMA. GMA, glycerol monomethacrylate; PEGA, poly(ethylene glycol) acrylate.

(Supplementary Table 10 and Supplementary Fig. 7). In contrast, when styrene was instead polymerized in the presence and the absence of acid, no rate enhancement was observed, as expected from a monomer that has no propensity to protonate (Supplementary Fig. 8 and Supplementary Table 11). Taken altogether, these data confirm the dual role of acid to not only effectively trigger the initiation but also to enhance the polymerization rate, therefore requiring a lower overall radical

concentration to reach comparable conversions, which subsequently results in less termination and narrower molar mass distributions.

The scope of acid-triggered RAFT polymerization
To expand the scope of this study, we subsequently investigated the compatibility of our approach with various monomers, RAFT agents, solvents and acids. Firstly, we switched from DMA to NAM utilizing

the commercially available RAFT agent 3-((((1-carboxyethyl)thio)carbonothioyl)thio)propanoic acid (CTA 2). A well-defined PNAM was obtained in aqueous media with $Đ = 1.13$, as seen in Supplementary Fig. 9 and Supplementary Table 12. A well-controlled acid-triggered RAFT polymerization was also observed in a range of polar solvents commonly employed for RAFT polymerization including dioxane, ethanol, dimethyl sulfoxide (DMSO) and acetonitrile resulting in polymers with narrow molar mass distributions ($Đ < 1.2$; Supplementary Fig. 9 and Supplementary Tables 12 and 13). Notably, the polymerization could also be successfully performed under bulk conditions without compromising the control over the reaction (Fig. 6b).

According to our preliminary DFT calculations, autoinitiation caused by monomer protonation is not exclusive to acrylamides but can in principle also occur with a wider range of monomer families such as acrylates, methacrylates and methacrylamides. Calculations demonstrating acid-catalysed autoinitiation of methyl methacrylate in dioxane (Supplementary Fig. 12) and DMSO (Supplementary Fig. 13), and of 2-methoxyethyl acrylate in water (Supplementary Fig. 14), are provided in Supplementary Information as examples. To investigate this scenario experimentally, poly(ethylene glycol) methyl ether acrylate (PEGA$_{480}$) was polymerized with dithiocarbamate methyl 2-[methyl(4-pyridinyl) carbamothioylthio]propionate (CTA 4) as the RAFT agent ($Đ = 1.18$; Fig. 6d and Supplementary Table 12). In a similar fashion, 2-cyanopropan-2-yl N-methyl-N-(pyridine-4-yl)carbamodithioate (CTA 5) was employed to polymerize N-(2-hydroxypropyl) methacrylamide (HPMA) with SEC, revealing a monomodal molar mass distribution $Đ = 1.19$ at very high monomer conversions (Fig. 6e and Supplementary Table 12). It is noted that this is a challenging monomer typically exhibiting much slower polymerization rates under previously reported literature conditions[50]. Glycerol monomethacrylate was chosen as a model methacrylic monomer, and upon polymerization using 4-((((2-carboxyethyl)thio)carbonothioyl)thio)-4-cyanopentanoic acid (CTA 3), a well-defined PGMA ($Đ = 1.13$; Fig. 6f and Supplementary Table 12) was obtained. Interestingly, even the relatively hydrophobic methyl methacrylate could be polymerized in DMSO utilizing dithiobenzoate 2-cyano-2-propyl benzodithioate (CTA 6) as the RAFT agent ($Đ = 1.18$; Supplementary Fig. 9 and Supplementary Table 13). Last but not least, sulfuric acid was replaced with weaker and more biocompatible acids such as acetic acid and citric acid without compromising the control over the molar mass distributions (Fig. 6c, Supplementary Tables 12 and 13, and Supplementary Fig. 9). Taken altogether, these experiments highlight the robustness and the versatility of our acid-triggered RAFT polymerization to successfully operate under a range of different monomer classes, RAFT agents, solvents and acids.

Conclusion

To summarize, we have presented an acid-triggered RAFT polymerization that operates in the absence of light and exogenous thermal radical initiators such as peroxides and azo-compounds. Using small amounts of either strong or weak acids, well-defined polymers can be obtained with excellent control over the molecular weight and dispersity. The method was successfully applied to a range of monomer classes (for example, (meth)acrylates and (meth)acrylamides), solvents (for example, DMSO, dioxane, acetonitrile and water) and RAFT agents (for example, trithiocarbonates and dithiobenzoates) and was also compatible with conventional radical polymerization. The superiority of the acid-triggered RAFT over previous thermal approaches was demonstrated through the synthesis of homo and block copolymers with faster polymerization rates, narrower molar mass distributions and suppressed termination. Mechanistically, the reaction was proposed to proceed through a Flory-type autoinitiation mechanism triggered by monomer protonation resulting in radical generation. The protonation was also found to accelerate the polymerization rate, yielding polymers with improved end-group fidelity. We believe that this acid-triggered polymerization will emerge as a powerful alternative to conventional thermal RAFT and FRP.

Methods

Synthesis of PDMA homopolymer with DP 500 in water with H$_2$SO$_4$

In a 5-ml vial, 9.24 mg (38.8 µmol, 1 equiv.) of PABTC (CTA 1) was added and dissolved in 2 ml of DMA (19.4 mmol, 500 equiv.), and then 1 ml of water was added. Subsequently, 21.57 µl of sulfuric acid (0.39 mmol, 10 equiv.) and a stirrer bar was added. The solution was purged with nitrogen for 15 min, and then the polymerization was conducted in an oil bath at 70 °C for 10 h with a 350 r.p.m. stirring rate to reach a conversion of 90% by ^{1}H NMR spectroscopy.

Kinetics of PDMA homopolymer with DP 500 in deuterated water (pH 1.7)

In a 5-ml vial, 4.6 mg (1 equiv.) of PABTC (CTA 1) was added and dissolved in 1 ml of DMA (500 equiv.), and then 4 ml of D$_2$O with 10 µl of H$_2$SO$_4$ (18 M, 10 equiv.) was added. An aliquot of 500 µl was transferred to an NMR tube and sealed with a septum. The solution was purged with nitrogen for 8 min in an ice bath. The polymerization was then conducted in the NMR (Bruker 400) that had been stabilized at 70 °C beforehand.

Synthesis of triblock copolymer with DP 200 per block in water with acid

In a 5-ml vial, 18.5 mg of CTA 2 (73.0 µmol, 1 equiv.) was dissolved in 1.50 ml of DMA (14.55 mmol, 200 equiv.). Subsequently, 0.74 ml of water and 4 µl of sulfuric acid (72.7 µmol, 1 equiv.) were added and a stirrer bar was inserted into the reaction vial. The vial was then sealed with a septum, before deoxygenation by nitrogen bubbling for 15 min. Polymerization was conducted in an oil bath at 70 °C for 20 h with a 200 r.p.m. stirring rate, to reach a conversion of 96% by ^{1}H NMR spectroscopy. In a separate vial, 1.83 ml (14.55 mmol, 200 equiv.) of NAM, 1.03 ml of water and 8 µl of sulfuric acid (145.4 µmol, 2 equiv.) were added and degassed under nitrogen atmosphere for 15 min before addition to the polymerization mixture via a nitrogen-purged syringe. The polymerization was left to proceed for 40 h, yielding a diblock copolymer ($Đ = 1.14$). Similarly, a third aliquot was prepared containing 1.50 ml of DMA (14.55 mmol, 200 equiv.), 0.67 ml of water and 12 µl of sulfuric acid (218.1 µmol, 3 equiv.), and was deoxygenated for 15 min. Then, the aliquot was added to the polymerization solution and the reaction was left to proceed for 24 h at 70 °C and then for 3 h at 80 °C, yielding a triblock copolymer with 94% conversion by ^{1}H NMR spectroscopy and $Đ = 1.16$.

Kinetics of PDMA synthesized via FRP in deuterated water (pH 1.3)

In a 5-ml vial, 1 ml of DMA was inserted, and then 4 ml D$_2$O with 10 µl H$_2$SO$_4$ (18 M) was added. An aliquot of 500 µl was transferred to an NMR tube and sealed with a septum. The solution was purged with nitrogen for 8 min in an ice bath. The polymerization was then conducted in the NMR (Bruker 400) that had been stabilized at 70 °C beforehand.

Computational procedures

Geometry optimizations of all equilibrium and transition structures of interest along the potential energy surfaces of the catalysed and uncatalysed self-initiation and propagation processes in water were performed at the M062X (ref. 51)/6-31g(d,p) level of theory using the 'solvent model - density' (SMD)[52] solvent model and an explicit water molecule. Frequency calculations at the same level of theory were employed to confirm equilibrium structures as having all real harmonic frequencies and transition structures as having a single imaginary frequency. Intrinsic reaction coordinate calculations[53] were further employed to verify the connectivities of the optimized transition structures to the respective minima of interest. To obtain more accurate electronic energies, single point energy calculations in implicit water were performed at the wB97X-D (ref. 54)/aug-cc-pVTZ level of theory with the SMD solvent model. Gibbs free energies were calculated using

the 'direct method'[55] in which ideal gas partition functions were applied to the solution-phase geometries and frequencies, and include a correction for the change of state from 1 atm to 1 M (ref. 56). All geometry optimizations, frequency, intrinsic reaction coordinate and single point energy calculations were performed using the Gaussian 16 software package[57], three-dimensional representations of chemical structures were generated using CYLview[58], and thermochemistry data were calculated with the aid of the Shermo program[59].

Data availability

The authors declare that the data to support the findings of this study are available within the paper and its Supplementary Information. Source data are provided with this paper.

References

1. Matyjaszewski, K. Atom transfer radical polymerization (ATRP): current status and future perspectives. *Macromolecules* **45**, 4015–4039 (2012).
2. Wang, J.-S. & Matyjaszewski, K. Controlled/'living' radical polymerization. Atom transfer radical polymerization in the presence of transition-metal complexes. *J. Am. Chem. Soc.* **117**, 5614–5615 (1995).
3. Kato, M., Kamigaito, M., Sawamoto, M. & Higashimura, T. Polymerization of methyl methacrylate with the carbon tetrachloride/dichlorotris-(triphenylphosphine)ruthenium (II)/ methylaluminum bis(2,6-di-*tert*-butylphenoxide) initiating system: possibility of living radical polymerization. *Macromolecules* **28**, 1721–1723 (1995).
4. Harth, E., Bosman, A. & Hawker, C. New polymer synthesis by nitroxide mediated living radical polymerization. *Chem. Rev.* **101**, 3661–3688 (2001).
5. Chiefari, J. et al. Living free-radical polymerization by reversible addition–fragmentation chain transfer: the RAFT process. *Macromolecules* **31**, 5559–5562 (1998).
6. Truong, N. P., Jones, G. R., Bradford, K. G., Konkolewicz, D. & Anastasaki, A. A comparison of RAFT and ATRP methods for controlled radical polymerization. *Nat. Rev. Chem.* **5**, 859–869 (2021).
7. Parkatzidis, K., Wang, H. S., Truong, N. P. & Anastasaki, A. Recent developments and future challenges in controlled radical polymerization: a 2020 update. *Chem* **6**, 1575–1588 (2020).
8. Antonopoulou, M.-N. et al. Concurrent control over sequence and dispersity in multiblock copolymers. *Nat. Chem.* **14**, 304–312 (2022).
9. Whitfield, R. et al. Tailoring polymer dispersity and shape of molecular weight distributions: methods and applications. *Chem. Sci.* **10**, 8724–8734 (2019).
10. Engelis, N. G. et al. Sequence-controlled methacrylic multiblock copolymers: expanding the scope of sulfur-free RAFT. *Macromolecules* **51**, 336–342 (2018).
11. Keddie, D. J., Moad, G., Rizzardo, E. & Thang, S. H. RAFT agent design and synthesis. *Macromolecules* **45**, 5321–5342 (2012).
12. Perrier, S. 50th anniversary perspective: RAFT polymerization—a user guide. *Macromolecules* **50**, 7433–7447 (2017).
13. Keddie, D. J. A guide to the synthesis of block copolymers using reversible-addition fragmentation chain transfer (RAFT) polymerization. *Chem. Soc. Rev.* **43**, 496–505 (2014).
14. Lorandi, F., Fantin, M. & Matyjaszewski, K. Atom transfer radical polymerization: a mechanistic perspective. *J. Am. Chem. Soc.* **144**, 15413–15430 (2022).
15. Goto, A. & Fukuda, T. Kinetics of living radical polymerization. *Prog. Polym. Sci.* **29**, 329–385 (2004).
16. Gody, G., Zetterlund, P. B., Perrier, S. & Harrisson, S. The limits of precision monomer placement in chain growth polymerization. *Nat. Commun.* **7**, 10514 (2016).
17. Gody, G., Maschmeyer, T., Zetterlund, P. B. & Perrier, S. Rapid and quantitative one-pot synthesis of sequence-controlled polymers by radical polymerization. *Nat. Commun.* **4**, 2505 (2013).
18. Chi, J.-H., Wu, S.-H. & Shu, C.-M. Thermal explosion analysis of methyl ethyl ketone peroxide by non-isothermal and isothermal calorimetric applications. *J. Hazard. Mater.* **171**, 1145–1149 (2009).
19. Liu, S.-H., Chen, Y.-C. & Hou, H.-Y. Thermal runaway hazard studies for ABVN mixed with acids or alkalines by DSC, TAM III, and VSP2. *J. Therm. Anal. Calorim.* **122**, 1107–1116 (2015).
20. Li, X.-R., Wang, X.-L. & Koseki, H. Study on thermal decomposition characteristics of AIBN. *J. Hazard. Mater.* **159**, 13–18 (2008).
21. Wu, X. et al. Thermal safety performance evaluation for typical free radical polymerization initiator of *tert*-butyl peroxypivalate. *ChemistrySelect* **5**, 10835–10840 (2020).
22. Nothling, M. D. et al. Progress and perspectives beyond traditional RAFT polymerization. *Adv. Sci.* **7**, 2001656 (2020).
23. Xu, J., Jung, K., Atme, A., Shanmugam, S. & Boyer, C. A robust and versatile photoinduced living polymerization of conjugated and unconjugated monomers and its oxygen tolerance. *J. Am. Chem. Soc.* **136**, 5508–5519 (2014).
24. Hartlieb, M. Photo-iniferter RAFT polymerization. *Macromol. Rapid Commun.* **43**, 2100514 (2022).
25. Carmean, R. N., Becker, T. E., Sims, M. B. & Sumerlin, B. S. Ultra-high molecular weights via aqueous reversible-deactivation radical polymerization. *Chem* **2**, 93–101 (2017).
26. Lehnen, A.-C., Kurki, J. A. & Hartlieb, M. The difference between photo-iniferter and conventional RAFT polymerization: high livingness enables the straightforward synthesis of multiblock copolymers. *Polym. Chem.* **13**, 1537–1546 (2022).
27. Kwak, Y. & Matyjaszewski, K. Effect of initiator and ligand structures on ATRP of styrene and methyl methacrylate initiated by alkyl dithiocarbamate. *Macromolecules* **41**, 6627–6635 (2008).
28. Kwak, Y., Nicolaÿ, R. & Matyjaszewski, K. Concurrent ATRP/RAFT of styrene and methyl methacrylate with dithioesters catalyzed by copper (I) complexes. *Macromolecules* **41**, 6602–6604 (2008).
29. Kwak, Y., Nicolaÿ, R. & Matyjaszewski, K. Synergistic interaction between ATRP and RAFT: taking the best of each world. *Aust. J. Chem.* **62**, 1384–1401 (2009).
30. Nicolaÿ, R., Kwak, Y. & Matyjaszewski, K. A green route to well-defined high-molecular-weight (co)polymers using ARGET ATRP with alkyl pseudohalides and copper catalysis. *Angew. Chem. Int. Ed.* **122**, 551–554 (2010).
31. Destarac, M. Industrial development of reversible-deactivation radical polymerization: is the induction period over? *Polym. Chem.* **9**, 4947–4967 (2018).
32. Destarac, M. Controlled radical polymerization: industrial stakes, obstacles and achievements. *Macromol. React. Eng.* **4**, 165–179 (2010).
33. Moad, G., Rizzardo, E. & Thang, S. H. RAFT polymerization and some of its applications. *Chem. Asian J.* **8**, 1634–1644 (2013).
34. Niu, J. et al. Rapid visible light-mediated controlled aqueous polymerization with in situ monitoring. *ACS Macro Lett.* **6**, 1109–1113 (2017).
35. Gody, G., Maschmeyer, T., Zetterlund, P. B. & Perrier, S. B. Pushing the limit of the RAFT process: multiblock copolymers by one-pot rapid multiple chain extensions at full monomer conversion. *Macromolecules* **47**, 3451–3460 (2014).
36. Lebreton, P. & Boutevin, B. Primary radical termination and unimolecular termination in the heterogeneous polymerization of acrylamide initiated by a fluorinated azo-derivative initiator: a kinetic study. *J. Polym. Sci. Part A* **38**, 1834–1843 (2000).
37. Srinivasan, S., Lee, M. W., Grady, M. C., Soroush, M. & Rappe, A. M. Self-initiation mechanism in spontaneous thermal polymerization of ethyl and *n*-butyl acrylate: a theoretical study. *J. Phys. Chem. A* **114**, 7975–7983 (2010).

38. Aoshima, S. & Kanaoka, S. A renaissance in living cationic polymerization. *Chem. Rev.* **109**, 5245–5287 (2009).

39. Srinivasan, S., Lee, M. W., Grady, M. C., Soroush, M. & Rappe, A. M. Computational study of the self-initiation mechanism in thermal polymerization of methyl acrylate. *J. Phys. Chem. A* **113**, 10787–10794 (2009).

40. Flory, P. J. The mechanism of vinyl polymerizations. *J. Am. Chem. Soc.* **59**, 241–253 (1937).

41. Lingnau, J., Stickler, M. & Meyerhoff, G. The spontaneous polymerization of methyl methacrylate-IV: formation of cyclic dimers and linear trimers. *Eur. Polym. J.* **16**, 785–791 (1980).

42. Gryn'ova, G., Marshall, D. L., Blansby, S. J. & Coote, M. L. Switching radical stability by pH-induced orbital conversion. *Nat. Chem.* **5**, 474–481 (2013).

43. Jiang, J. Y., Smith, L. M., Tyrell, J. H. & Coote, M. L. Pulsed laser polymerisation studies of methyl methacrylate in the presence of $AlCl_3$ and $ZnCl_2$—evidence of propagation catalysis. *Polym. Chem.* **8**, 5948–5953 (2017).

44. Ciampi, S., Darwish, N., Aitken, H. M., Díez-Pérez, I. & Coote, M. L. Harnessing electrostatic catalysis in single molecule, electrochemical and chemical systems: a rapidly growing experimental tool box. *Chem. Soc. Rev.* **47**, 5146–5164 (2018).

45. Isobe, Y., Nakano, T. & Okamoto, Y. Stereocontrol during the free-radical polymerization of methacrylates with Lewis acids. *J. Polym. Sci. Part A* **39**, 1463–1471 (2001).

46. Noble, B. B., Smith, L. M. & Coote, M. L. The effect of LiNTf2 on the propagation rate coefficient of methyl methacrylate. *Polym. Chem.* **5**, 4974–4983 (2014).

47. Clark, T. Radical addition to alkene–metal cation complexes. *J. Chem. Soc. Chem. Commun.* https://doi.org/10.1039/c39860001774 (1986).

48. Vyakaranam, K., Barbour, J. B. & Michl, J. Li^+-catalyzed radical polymerization of simple terminal alkenes. *J. Am. Chem. Soc.* **128**, 5610–5611 (2006).

49. Luo, R. & Sen, A. Rate enhancement in controlled radical polymerization of acrylates using recyclable heterogeneous Lewis acid. *Macromolecules* **40**, 154–156 (2007).

50. Scales, C. W., Vasilieva, Y. A., Convertine, A. J., Lowe, A. B. & McCormick, C. L. Direct, controlled synthesis of the nonimmunogenic, hydrophilic polymer, poly(N-(2-hydroxypropyl) methacrylamide) via RAFT in aqueous media. *Biomacromolecules* **6**, 1846–1850 (2005).

51. Zhao, Y. & Truhlar, D. G. The M06 suite of density functionals for main group thermochemistry, thermochemical kinetics, noncovalent interactions, excited states, and transition elements: two new functionals and systematic testing of four M06-class functionals and 12 other functionals. *Theor. Chem. Acc.* **120**, 215–241 (2008).

52. Marenich, A. V., Cramer, C. J. & Truhlar, D. G. Universal solvation model based on solute electron density and on a continuum model of the solvent defined by the bulk dielectric constant and atomic surface tensions. *J. Phys. Chem. B* **113**, 6378–6396 (2009).

53. Gonzalez, C. & Schlegel, H. B. An improved algorithm for reaction path following. *J. Chem. Phys.* **90**, 2154–2161 (1989).

54. Chai, J.-D. & Head-Gordon, M. Long-range corrected hybrid density functionals with damped atom–atom dispersion corrections. *Phys. Chem. Chem. Phys.* **10**, 6615–6620 (2008).

55. Ribeiro, R. F., Marenich, A. V., Cramer, C. J. & Truhlar, D. G. Use of solution-phase vibrational frequencies in continuum models for the free energy of solvation. *J. Phys. Chem. B* **115**, 14556–14562 (2011).

56. Ho, J., Klamt, A. & Coote, M. L. Comment on the correct use of continuum solvent models. *J. Phys. Chem. A* **114**, 13442–13444 (2010).

57. *Gaussian 16 Rev. C.01* (Gaussian, 2016).

58. *CYLview* (Université de Sherbrooke, 2009).

59. Lu, T. & Chen, Q. Shermo: a general code for calculating molecular thermochemistry properties. *Comput. Theor. Chem.* **1200**, 113249 (2021).

Acknowledgements

Author contributions

A.A. managed and directed the overall project and together with N.P.T. co-supervised the experimental work; M.-N.A. discovered the acid-triggered polymerization, and performed the vast majority of the experiments. G.R.J. also performed selected experiments. M.-N.A and G.R.J. analysed the data with input from A.A. and N.P.T. M.L.C. managed the theoretical work of the project and was also instrumental in data analysis and discussions. A.A.K. and Z.P. conducted the DFT calculations supervised by M.L.C. M.-N.A. and A.A. co-wrote the manuscript with input from G.R.J., N.P.T. and M.L.C. All the authors discussed the results and commented on the manuscript.

Funding

Open access funding provided by Swiss Federal Institute of Technology Zurich.

Competing interests

The authors declare no competing interests.

Additional information

Supplementary information The online version contains supplementary material available at https://doi.org/10.1038/s44160-023-00462-9.

Correspondence and requests for materials should be addressed to Michelle L. Coote, Nghia P. Truong or Athina Anastasaki.

Peer review information *Nature Synthesis* thanks the anonymous reviewers for their contribution to the peer review of this work. Primary Handling Editor: Alison Stoddart, in collaboration with the *Nature Synthesis* team.

Reprints and permissions information is available at www.nature.com/reprints.

Publisher's note Springer Nature remains neutral with regard to jurisdictional claims in published maps and institutional affiliations.